

Local Controllability of Magnetized Purcell's Swimmers

Clément Moreau*

* *Université Côte d'Azur, Inria Sophia Antipolis, McTAO team,
 France (e-mail: clement.moreau@inria.fr).*

Abstract: We focus on the control theory aspects of the dynamics of magnetized micro-swimmer robots made of two or three rigid links. Under generic assumptions on the parameters, we show that the control system which models the swimmers' dynamics is locally controllable in small time around its equilibrium position (the straight line), but with bounded controls that do not go to zero as the target state gets closer to the initial state. Numerical simulations illustrate the results, which are relevant for useful applications in the micro-swimming field.

Keywords: Control theory, micro-swimming, robotics

1. INTRODUCTION

Micro-swimming robots offer potential high-impact applications in the biomedical field, such as targeted drug delivery or non-invasive surgery. For that reason, the interest in building such robots has been growing in the past years. The shapes and propulsion techniques of these new robots could be inspired by biology, since micro-organisms such as sperm cells or bacteria developed efficient ways to move through a surrounding fluid (see Peyer et al. (2013)). One promising technique consists of using an external magnetic field to drive a magnetized swimmer (see Gao et al. (2012); Dreyfus et al. (2005); Ghosh and Fischer (2009)).

Here, we focus on this type of propulsion, applied on simple models of micro-swimmers consisting of two or three magnetized segments linked by elastic joints. Such models, with different numbers of segments, have been studied for instance in the works of Gutman and Or (2014) and Alouges et al. (2013), in which the authors show that sinusoidal magnetic fields allow the swimmer to move forward in a prescribed direction. The 3-link articulated swimmer was introduced by Purcell in a founding talk about micro-swimming (see Purcell (1977)).

At the microscopic scale, the Reynolds number is typically very small (around 10^{-6}), which means that the intensity of inertial forces is negligible compared to those of viscous ones. Therefore, we can assume that the fluid is governed by the Stokes equations. We model the hydrodynamic interaction between the swimmer and the fluid by the local drag approximation of Resistive Force Theory introduced in the work of Gray and Hancock (1955).

We state a local controllability result for the 2- and 3-link swimmers. Under generic conditions on the links magnetizations, they are controllable around their equilibrium position (a straight line), but with controls that cannot be made arbitrarily small. This is due to the fact that the parallel component of the magnetic field cannot act on the swimmer when all its links are aligned. The results give an

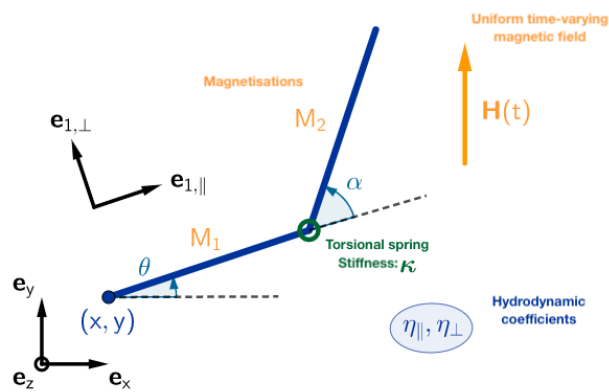


Fig. 1. Parametrization of the 2-link swimmer model

explicit bound on the controls to achieve small-time local controllability (STLC).

This extended abstract reproduces the model and results developed in Moreau (2019); Giraldi et al. (2019), without going into detailed derivation of the equations and proofs of the results, for the sake of brevity. It features new numerical simulations for the three-link swimmer, that illustrate its controllability properties in the general case and in a degenerate case that was left open in Moreau (2019).

2. THE MODEL

2.1 The swimmers

We mostly follow the notations and model used in the works of Alouges et al. (2015), Giraldi and Pommet (2017) and Giraldi et al. (2016). We focus on micro-swimmers consisting of two or three rigid magnetized segments – see Figures 1 and 2 – connected by torsional springs with stiffness κ , and subject to a uniform in space, time-varying magnetic field \mathbf{H} . The segments, called S_i with $i = 1, 2$ or 3 , have same length l , same hydrodynamic drag coefficients ξ and η , and magnetic moments M_i .

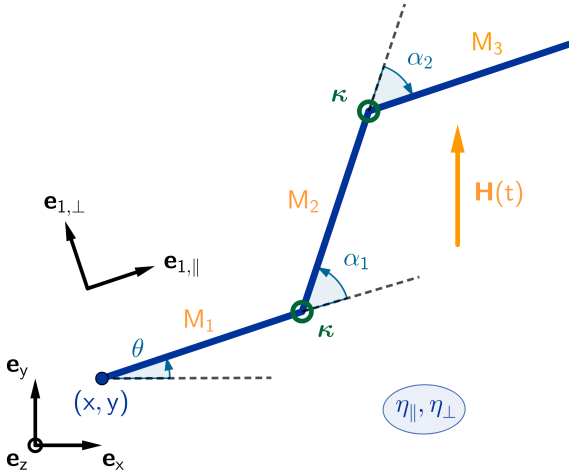


Fig. 2. Parametrization of the 3-link swimmer model

The swimmers can move in the 2d-plane defined by the vectors \mathbf{e}_x and \mathbf{e}_y . Let $\mathbf{e}_z = \mathbf{e}_x \times \mathbf{e}_y$. Let $\mathbf{x} = (x, y)$ be the coordinates of the end of S_1 , θ the angle between (Ox) and S_1 . In the two- (respectively three-)link case, we denote by α the angle between S_1 and S_2 (resp. by α_1 and α_2 the angles between S_1 and S_2 and between S_2 and S_3). The swimmer is then completely described by the four (resp. five) state variables $Z = (x, y, \theta, \alpha)$ (resp. $Z = (x, y, \theta, \alpha_1, \alpha_2)$): the pair (x, y) represents the position of the swimmer, θ its orientation and α (resp. (α_1, α_2)) its shape. Let us also define the moving frames associated to S_i for $i = 1, 2$ or 3 as $(\mathbf{e}_{i,\parallel}, \mathbf{e}_{i,\perp})$.

2.2 The control system

The magnetic field $\mathbf{H}(t)$ induces a torque in each of the segments. As it moves, the swimmer experiences hydrodynamic drag, as well as elastic restoring torques at the joints between the segments.

Elasticity The torsional springs which connect the swimmer segments exert a torque \mathbf{T}^{el} proportional to the shape angles α (resp. α_1 and α_2 for the 3-link model). Hence :

- for the 2-link swimmer, the torque \mathbf{T}^{el} exerted on S_2 is given by $\mathbf{T}_2^{\text{el}} = \kappa \alpha \mathbf{e}_z$;
- for the 3-link swimmer, the torque \mathbf{T}_2^{el} exerted on S_2 is given by $\mathbf{T}_2^{\text{el}} = \kappa \alpha_1 \mathbf{e}_z$ and the torque \mathbf{T}_3^{el} exerted on S_3 is given by $\mathbf{T}_3^{\text{el}} = \kappa \alpha_2 \mathbf{e}_z$.

The springs tend to get the swimmer back to a straight shape, in which all the segments are aligned.

Hydrodynamics The fluid surrounding the swimmer exerts a hydrodynamic drag on it. We use the Resistive Force Theory Gray and Hancock (1955) to model this interaction, i.e. the drag force per unit of length is proportional to the velocity and to the hydrodynamics coefficients ξ and η . For $s \in [0, \ell]$, let \mathbf{x}_s be the point of arclength s on one of the segments S_i . Its velocity $\mathbf{u}_i(\mathbf{x}_s)$ is given in the moving frame $(\mathbf{e}_{i,\parallel}, \mathbf{e}_{i,\perp})$ by $\mathbf{u}_i(\mathbf{x}_s) = u_{i,\parallel} \mathbf{e}_{i,\parallel} + u_{i,\perp} \mathbf{e}_{i,\perp}$. The drag force exerted on this point is then given by

$$\mathbf{f}_i(\mathbf{x}_s) = -\xi u_{i,\parallel} \mathbf{e}_{i,\parallel} - \eta u_{i,\perp} \mathbf{e}_{i,\perp}.$$

Integrating over S_i to obtain the total force \mathbf{F}_i^h exerted on S_i :

$$\mathbf{F}_i^h = \int_{S_i} \mathbf{f}_i(\mathbf{x}_s) d\mathbf{x}_s.$$

Moreover, given a point \mathbf{x}_0 , the drag torque for S_i with respect to \mathbf{x}_0 takes the form

$$\mathbf{T}_{i,\mathbf{x}_0}^h = \int_{S_i} (\mathbf{x}_s - \mathbf{x}_0) \times \mathbf{f}_i(\mathbf{x}_s) d\mathbf{x}_s.$$

Hydrodynamic drag effects are resistant: without a magnetic field, the swimmer tends to immobilize at its equilibrium straight shape.

Magnetism The magnetic field exerts a torque \mathbf{T}_i^m on S_i which is proportional to its magnetization coefficient M_i : $\mathbf{T}_i^m = M_i \mathbf{e}_{i,\parallel} \times \mathbf{H}$.

The swimmers are considered sufficiently small to be at low Reynolds number regime, and, as a result, inertia may be neglected (see Purcell (1977)). Writing the balance of forces and torques and expressing the different contributions F_i^h , T_i^h and T_i^m , we can write the dynamics of the swimmers as a nonlinear control system given by

$$\dot{Z} = \mathbf{F}_0 + H_{\parallel} \mathbf{F}_1 + H_{\perp} \mathbf{F}_2, \quad (1)$$

with H_{\parallel} and H_{\perp} the projection of the magnetic field in the moving frame associated to S_1 : $\mathbf{H}(t) = H_{\parallel} \mathbf{e}_{1,\parallel} + H_{\perp} \mathbf{e}_{1,\perp}$, and F_0 , F_1 and F_2 vector fields calculated from the system parameters. The magnetic components H_{\parallel} and H_{\perp} are seen as the control functions.

Moreover, $\mathbf{F}_0(0) = 0$ and $\mathbf{F}_1(0) = 0$, which means that if the orthogonal magnetic field is equal to zero, (i.e. $H_{\perp} = 0$ for all times), for any H_{\parallel} , states of the form $(x, y, \theta, 0)$ (resp. $(x, y, \theta, 0, 0)$ for the 3-link swimmer) with $(x, y, \theta) \in \mathbf{R}^3$ are equilibrium positions. Since the problem is invariant by translation and rotation, we focus on the equilibrium position $(0, 0, 0, 0)$ (resp. $(0, 0, 0, 0, 0)$), without loss of generality. In the following, we study local controllability of the swimmers around this equilibrium position, noted 0 for the sake of readability.

3. LOCAL CONTROLLABILITY AROUND EQUILIBRIUM STATES

We recall the definition of small-time local controllability that we will use later on. Let

$$\dot{z} = f_0(z) + u_1(t) f_1(z) + u_2(t) f_2(z). \quad (2)$$

be a general nonlinear control-affine system, with z in \mathbf{R}^n , f_0, f_1, f_2 real analytic vector fields in \mathbf{R}^n and u_1, u_2 control functions in $L^\infty([0, T])$ for some $T > 0$. For $\eta > 0$, and $z \in \mathbf{R}^n$, let $B(z, \eta)$ be the open ball centered at z with radius η . The following definition appears in (Coron, 2007, Definition 3.2).

Let z_e in \mathbf{R}^n , and $u_e = (u_{1e}, u_{2e})$ constant controls such that (z_e, u_e) is an equilibrium of the system (2). The control system (2) is *STLC* at (z_e, u_e) if, for every $\varepsilon > 0$, there exists $\zeta > 0$ such that, for every z_0, z_1 in $B(z_e, \zeta)$, there exists controls $u_1(\cdot)$ and $u_2(\cdot)$ in $L^\infty([0, \varepsilon])$ such that the solution of the control system $z(\cdot) : [0, \varepsilon] \rightarrow \mathbf{R}^n$ of (2) satisfies $z(0) = z_0$, $z(\varepsilon) = z_1$, and

$$\|u_1 - u_{1e}\|_{L^\infty} \leq \varepsilon, \|u_2 - u_{2e}\|_{L^\infty} \leq \varepsilon.$$

4. RESULTS FOR THE 2- AND 3-LINK SWIMMERS

From now on, we assume that the physical constants ℓ , η , ξ , κ are positive, and that $\eta > \xi$. This is usually true in the swimmer's physical setting (for thin filaments, one typically has $\eta = 2\xi$, see Gray and Hancock (1955)), and avoid dealing with numerous subcases.

4.1 The 2-link case

Before stating the result, we need to make a few technical assumptions about the magnetizations.

Assumption 1. The magnetizations M_1 , and M_2 are such that $M_1 \neq 0$, $M_2 \neq 0$, $M_1 - M_2 \neq 0$ and $M_1 + M_2 \neq 0$.

Remark 1. It can be shown that the swimmer is not STLC at $(0, (0, 0))$ if $M_1 = 0$, $M_2 = 0$ or $M_1 - M_2 = 0$, and that it is STLC at $(0, (0, 0))$ if $M_1 + M_2 = 0$.

Theorem 1. The two-link swimmer is STLC at $(0, (\gamma_2, 0))$ with

$$\gamma_2 = \kappa \left(\frac{1}{M_1} + \frac{1}{M_2} \right).$$

Moreover, it is not STLC at $(0, (\alpha, 0))$ with $\alpha \neq \gamma_2$.

4.2 The 3-link case

Let $m = M_1 + M_3$ and $\mu = M_1 - M_3$.

Assumption 2. The magnetizations M_1 , M_2 and M_3 are such that

$$\begin{aligned} & \mu \neq 0; \\ & (m \neq 0 \text{ or } M_2 \neq 0); \\ & -7M_2^2 + 9M_2m - 5M_1M_3 \neq 0; \\ & P(M_1, M_2, M_3) \neq 0, \end{aligned} \quad (3)$$

with

$$\begin{aligned} P(x, y, z) = & 49y^3 - 91y^2(x + z) \\ & + 36y(x + z)^2 - (45y + 65(x + z))xz. \end{aligned}$$

Remark 2. It can be shown that the first three conditions in equation (3) are necessary for local controllability. It is unclear whether the last one is also necessary. The polynomial expression P seems to be of importance in the swimmer's dynamics, as it appears in all the calculations needed in the proof of Theorem 2 below. The values of (M_1, M_2, M_3) for which P vanishes may correspond with cases where the swimmer's movement ability is limited. We conducted numerical simulations, displayed on Figure 4 below, that tend to confirm this hypothesis.

Theorem 2. The three-link swimmer is STLC at $(0, (\gamma_3, 0))$ with

$$\gamma_3 = \kappa \frac{17m - 16M_2}{-7M_2^2 + 9M_2m - 5M_1M_3}.$$

Moreover, it is not STLC at $(0, (\alpha, 0))$ with $\alpha \neq \gamma_3$.

5. COMMENTS ON THE RESULTS. PERSPECTIVES

Theorems 1 and 2 provide a full understanding of the local controllability properties of the magnetically actuated 2- and 3-link swimmers. They show, rather counterintuitively, that the parallel component of the magnetic field needs to remain large in order to control the swimmer, even when the target state is very close to its equilibrium position. In some particular cases, such as $16m - 17M_2 = 0$

in the three-link case, the constant γ_3 is equal to 0, and the standard STLC at $(0, (0, 0))$ is retrieved.

Physically, these results reflect the fact that the parallel component of the magnetic field has no effect on the swimmer when it is at its equilibrium shape, i.e. when all the segments are aligned. This may be seen as a loss of controllability at the equilibrium. The parallel control H_{\parallel} plays however a crucial role in the controllability properties of the swimmers.

This result provides a useful insight for experiments, by showing that the 2- and 3-link swimmers may not be driven easily in any direction from an equilibrium point, and giving an explicit lower bound on the control needed to achieve local controllability. Further work on the subject of micro-swimmers, currently under our investigation, is to consider swimmers with more links, that describe more realistically flexible filaments. This work also addresses the question of the existence of necessary conditions for local controllability for systems with non-scalar controls, for which little is known.

6. NUMERICAL SIMULATIONS FOR THE 2-LINK SWIMMER

In order to numerically observe the local behavior of the system, we steer it from an equilibrium state with different controls that stay "close" to the equilibrium control. Let β be a real number and $\epsilon > 0$ be a small parameter; we set

$$\begin{aligned} H_{\parallel}(t) &= \beta + \epsilon(h_1 + h_2 \cos(10t) + h_3 \cos(100t)) \\ H_{\perp}(t) &= \epsilon(h_4 + h_5 \cos(10t) + h_6 \cos(100t)) \end{aligned} \quad (4)$$

with h_1 to h_6 constants taken randomly in $[-1, 1]$. We take N realizations of these random controls and solve the 2- and 3-link swimmer systems, starting respectively from $(0, 0, 0, 0)$ and $(0, 0, 0, 0, 0)$ over the time interval $[0, T]$. With such a range of randomized oscillating controls close to $(\beta, 0)$, we expect the obtained trajectories to roughly cover the reachable space in small time T , which allows to observe the unattainable regions if there are any. The results of the simulations, performed with MATLAB, are displayed on Figure 3 for the 2-link swimmer and on Figure 4 for the 3-link swimmer. When β is different from the critical values γ_2 and γ_3 , the trajectories remain, locally, either always left or always right of $(0, 0)$ in the 2d-plane, which tends to validate the non-STLC of the swimmer. On the contrary, for $\beta = \gamma_2$ or $\beta = \gamma_3$, the trajectories cover a neighborhood of 0.

The bottom row of Figure 4 gives insight as to why the last condition in equation (3) is necessary for the 3-link swimmer controllability. It shows that, if $P(M_1, M_2, M_3) = 0$ and $\beta = \gamma_3$, then α_1 remains approximately equal to α_2 for all time, which suggests that the swimmer's movement ability might be limited in this particular case.

ACKNOWLEDGEMENTS

The author thanks Laetitia Giraldi, Pierre Lissy and Jean-Baptiste Pomet for their invaluable help and advice that greatly assisted the research.

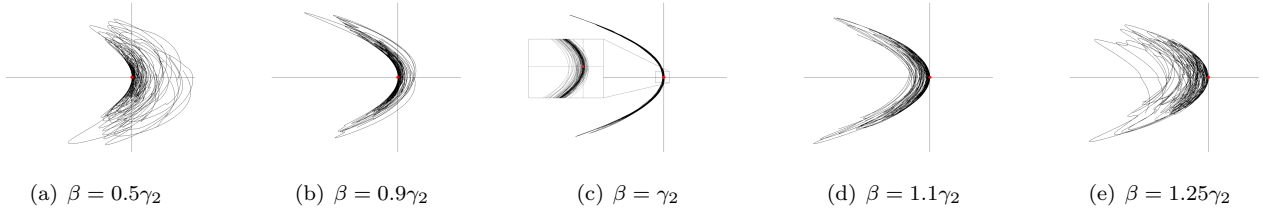


Fig. 3. Illustration of the role played by the constant γ_2 for the two-link swimmer. On each graph are plotted $N = 30$ trajectories of the swimmer’s extremity in the 2d-plane (x, y) , with the randomized controls (4) taken “around” $(\beta, 0)$, for 5 different values of β (a zoom-in around the origin is added on the middle graph). The origin $(0, 0)$ is indicated by the red dot on each graph. When β is different from the critical value γ_2 , the trajectories remain either all to the left or all to the right of the origin. Only the control $(\gamma_2, 0)$ enables the trajectories to cover a neighbourhood of the origin. Numerical values: $\eta = 4$, $\xi = 2$, $l = 1$, $M_1 = 1$, $M_2 = 3$, $k = 1$, $\varepsilon = 10^{-2}$, $T = 1$.

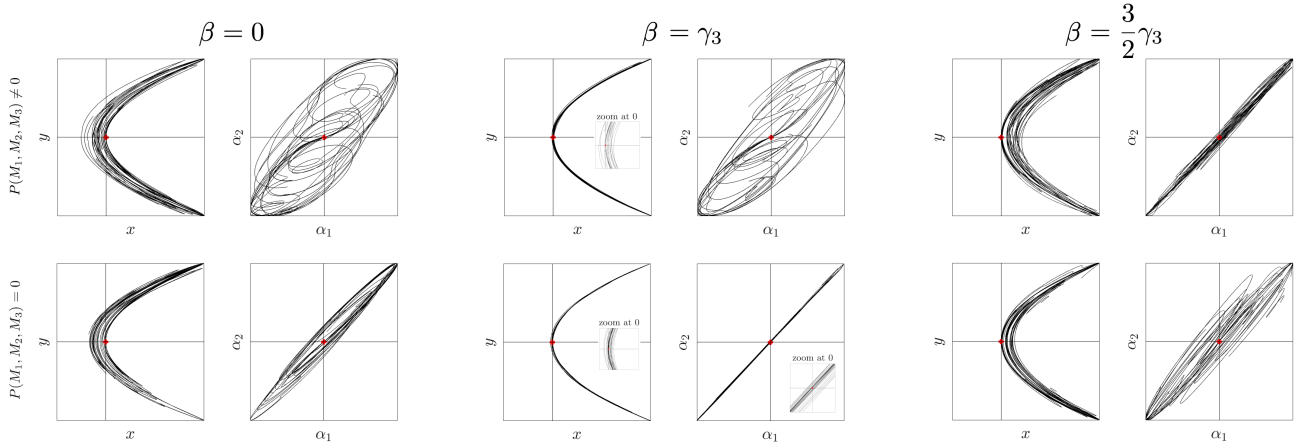


Fig. 4. Illustration of the role played by the constant γ_3 for the three-link swimmer. On each couple of plots, the evolution of (x, y) and (α_1, α_2) for $N = 15$ trajectories has been drawn with realisations of controls (4) taken “around” $(\beta, 0)$ for three different values of β (zoom-ins around the origin are occasionally added). When β is different from the critical value γ_3 , the trajectories remain either all to the left or all to the right of the origin. Only the control $(\gamma_3, 0)$ enables the trajectories to cover a neighbourhood of the origin. The second row of plots illustrates the change in the swimmer’s behaviour in the (α_1, α_2) plane when $\beta = \gamma_3$ and $P(M_1, M_2, M_3) = 0$. Numerical values: $\eta = 4$, $\xi = 2$, $l = 1$, $M_1 = 8$ (first row), $M_1 = 7.069$ (second row), $M_2 = 10$, $M_3 = 4$, $k = 1$, $\varepsilon = 10^{-2}$, $T = 1$.

REFERENCES

Alouges, F., DeSimone, A., Giraldi, L., and Zoppello, M. (2013). Self-propulsion of slender micro-swimmers by curvature control: N-link swimmers. *International Journal of Non-Linear Mechanics*, 56, 132–141.

Alouges, F., DeSimone, A., Giraldi, L., and Zoppello, M. (2015). Can magnetic multilayers propel artificial microswimmers mimicking sperm cells? *Soft Robotics*, 2(3), 117–128.

Coron, J.M. (2007). *Control and nonlinearity*, volume 136 of *Mathematical Surveys and Monographs*. AMS, Providence, RI.

Dreyfus, R., Baudry, J., Roper, M.L., Fermigier, M., Stone, H.A., and Bibette, J. (2005). Microscopic artificial swimmers. *Nature*, 437(7060), 862.

Gao, W., Kagan, D., Pak, O.S., Clawson, C., Campuzano, S., Chuluun-Erdene, E., Shipton, E., Fullerton, E.E., Zhang, L., Lauga, E., et al. (2012). Cargo-towing fuel-free magnetic nanoswimmers for targeted drug delivery. *small*, 8(3), 460–467.

Ghosh, A. and Fischer, P. (2009). Controlled propulsion of artificial magnetic nanostructured propellers. *Nano letters*, 9(6), 2243–2245.

Giraldi, L., Lissy, P., Moreau, C., and Pomet, J.B. (2016). Controllability of a bent 3-link magnetic microswimmer. *arXiv preprint arXiv:1611.00993*.

Giraldi, L., Lissy, P., Moreau, C., and Pomet, J.B. (2019). Necessary conditions for local controllability of a particular class of systems with two scalar controls. *arXiv preprint arXiv:1907.04706*.

Giraldi, L. and Pomet, J.B. (2017). Local controllability of the two-link magneto-elastic micro-swimmer. *IEEE Transactions on Automatic Control*, 62(5), 2512–2518.

Gray, J. and Hancock, G. (1955). The propulsion of sea-urchin spermatozoa. *Journal of Experimental Biology*, 32(4), 802–814.

Gutman, E. and Or, Y. (2014). Simple model of a planar undulating magnetic microswimmer. *Physical Review E*, 90(1), 013012.

Moreau, C. (2019). Local controllability of a magnetized purcell’s swimmer. *IEEE Control Systems Letters*, 3(3), 637–642.

Peyer, K.E., Zhang, L., and Nelson, B.J. (2013). Bio-inspired magnetic swimming microrobots for biomedical applications. *Nanoscale*, 5(4), 1259–1272.

Purcell, E.M. (1977). Life at low reynolds number. *American journal of physics*, 45(1), 3–11.